Adsorption (2013) 19:529–535
DOI 10.1007/s10450-013-9475-x

What can positronium tell us about adsorption?

Agnieszka Kierys · Radosław Zaleski · Maciej Tydda · Jacek Goworek

Received: 10 November 2012 / Accepted: 16 January 2013 / Published online: 30 January 2013

Abstract The condensation and evaporation of *n*-heptane at 298 K in mesopores of silica material obtained by the polymer templating method have been studied by PALS measurements. It is demonstrated that the *ortho*-positronium lifetimes and intensities provide valuable information on pore filling and emptying which are not accessible from a conventional adsorption experiment. The results confirm the specific adsorption mechanism of *n*-heptane in pores with narrow openings (ink-bottle shape) which is different from that known for other pore geometries. The results from PALS experiment are compared to those derived from the conventional *n*-heptane and nitrogen adsorption data.

Keywords Silica gel · Positron annihilation lifetime spectroscopy (PALS) · *N*-heptane adsorption

1 Introduction

The pore structure of solids is of significant importance for their numerous applications. The most commonly used methods of pore characterization are those based on the meniscus curvature of the liquid filling the pores and the phase transitions within the pores. Gas adsorption experiments are the most popular and the standard approach to pore characterization. The results which are provided by the adsorption method strongly depend on the interpretation of the adsorption isotherms. Correct interpretation of the adsorption data requires complete and precise description of the related mechanisms (e.g., the adsorbate multilayer formation on the solid surface or adsorbate condensation). Generally, all types of phase transitions at different stages of adsorption must be known. Depending on the porosity type, the shape of pores and their interconnections, the mechanism of gas adsorption and desorption is different. Therefore, the filling of pores and their emptying are accompanied by pore blocking, cavitation, formation of free volumes at liquid–solid interface and changes of the liquid condensate density. The above mentioned factors make the interpretation of adsorption data quite complex. Thus, many other methods have been developed for investigations of the pore systems in solid materials (Brun et al. 1977; Goworek and Stefaniak 1992, 1994; Furtado et al. 2011; Krause et al. 2011; Pikus et al. 2010; Schüth et al. 2002; Smarsly et al. 2001). Recently, one of the most promising techniques for these purposes seems to be the method based on measurements of the positronium (i.e., bound state of positron and electron) annihilation lifetime. Positron annihilation lifetime spectroscopy (PALS) makes it possible to characterize of many types of free volumes within a wide range of pore sizes, regardless of whether they are present in solid or in liquid (Goworek et al. 1997, 1998, 2010; He et al. 2007; Koshimizu et al. 2008; Kullmann et al. 2010; Thraenert et al. 2007; Zaleski et al. 2003, 2011, 2012b Zgardzińska and Goworek 2010, 2012a, b).

The present paper focuses on PALS study of adsorption of *n*-heptane on silica gel derived from a polymer-silica composite. This silica material shows non-typical pore structure which results from the applied preparation procedure (Halasz et al. 2011; Zaleski et al. 2012a). The state of the adsorbate phase during successive stages of pore filling and pore

A. Kierys (✉) · J. Goworek
Department of Adsorption, Faculty of Chemistry,
Maria Curie-Sklodowska University,
Pl. M. Curie-Sklodowskiej 3, 20-031 Lublin, Poland
e-mail: agnieszka.kierys@umcs.lublin.pl

R. Zaleski · M. Tydda
Department of Nuclear Methods, Institute of Physics,
Maria Curie-Sklodowska University, Pl. M. Curie-Sklodowskiej
1, 20-031 Lublin, Poland

evacuation is deduced from PALS results. The observed effects are correlated with the basic characteristics derived from the conventional adsorption isotherms.

2 Experimental

2.1 Materials

The silica gel preparation, used in this experiment was in detail described earlier in references (Halasz et al. 2011; Zaleski et al. 2012a). The commercially available Amberlite XAD7HP supplied by ROHM and HAAS (now Dow Chemical Co.) was used as a polymer porous template. The polymer/silica composite was obtained after hydrolysis and condensation at pH = 0.44 of the silica source (tetraethoxysilane, TEOS, Sigma-Aldrich, 98 %) embedded in polymer beads. The spherically shaped silica gel particles without the organic substrate were prepared by calcination of the composite in air at 550 °C for 12 h.

2.2 Characterization methods

2.2.1 Low-temperature nitrogen adsorption

N_2 adsorption isotherms were measured at 77 K using Quantachrome 1CMS volumetric adsorption analyzer. The investigated sample was outgassed, prior to the adsorption measurements, for 12 h at 473 K. The standard BET method was used to evaluate the specific surface area. The total pore volume was determined from single point adsorption at $p/p_0 = 0.985$. The pore size distribution in the mesopore range was calculated by the NLDFT equilibrium model for cylindrical pore geometry using Quantachrome's proprietary Autosorb 1.51 software.

2.2.2 N-heptane adsorption

N-heptane adsorption isotherm on the investigated silica gel was measured at 293 K thanks to the courtesy of Micromeritics Instrument Corp. as a project PR120111-001, using ASAP 2020 V4.00 (V4.00 H) volumetric adsorption analyser.

2.2.3 SEM

SEM studies were conducted on FEI Quanta^{TM} 3D FEG microscope.

2.2.4 PALS

A standard "fast-slow" delayed coincidence spectrometer was used for positron annihilation lifetime spectra measurement. BaF_2 scintillators coupled with Photonis XP 2020Q photomultipliers, as well as wide energy windows assured a high detection efficiency. Over 1.7×10^7 coincidences in each spectrum were detected during 4 h using 0.5 MBq ^{22}Na positron source sealed in an 8 μm Kapton envelope. The efficiency was obtained at the expense of the resolution width. The resolution function had to be approximated by two Gaussians (their FWHMs were 285 and 413 ps and contribution of 72 and 28 %, respectively). LT9.2 program (Kansy 1996) as well as MELT program (Shukla et al. 1993; Zaleski 2006) were used for analysis of PALS spectra.

The gas dosing system was coupled with a vacuum chamber, where a sample-positron source-sample sandwich was placed. Before *n*-heptane introduction into the sample the degassing procedure was applied to the alkane three times. It consisted in freezing *n*-heptane in liquid nitrogen followed by pumping out impurities while *n*-heptane was slowly melting. Series of PALS measurements at various *n*-heptane pressures was conducted at room temperature.

3 Results and discussion

At first the investigated silica gel morphology and internal structure of the particle were probed by SEM. The results (not shown) confirm that the silica beads preserved a spherical shape of initial polymer and are mechanically stable after calcination and elimination of the polymer matrix. The very fine primary particles, having a diameter in the range from 6 to 10 nm, constituting the internal structure of the silica gel beads are very densely packed. It should be emphasized that the porosity of the investigated samples consists of irregular voids which are typically interconnected, between the irregularly aggregated primary particles.

The nitrogen and *n*-heptane adsorption isotherms on silica gel under study are given in Fig. 1, whereas the parameters characterizing the porosity of the investigated silica obtained from the low-temperature nitrogen adsorption experiment are as follows: the specific surface area, $S_{BET} = 1{,}135\ m^2/g$, the pore volume $V_p = 1.06\ cm^3/g$ and the average pore size $D_m = 4V_p/S_{BET} = 3.7$ nm. The parameters obtained from *n*-heptane adsorption experiment are: 706 m^2/g, 0.83 cm^3/g, 4.7 nm, respectively. A continuous and almost linear increase of nitrogen as well as *n*-heptane adsorption within a wide pressure range is observed for the discussed silica gel, which suggests that the pore sizes are irregular. The shape of the hysteresis loop present in the N_2 isotherms suggests the presence of ink-bottle or spherically shaped pores.

The pore size distributions (PSD) presented in Fig. 2 are of complex character and indicate that the pore sizes ranging from micro- to mesopores. Moreover, the

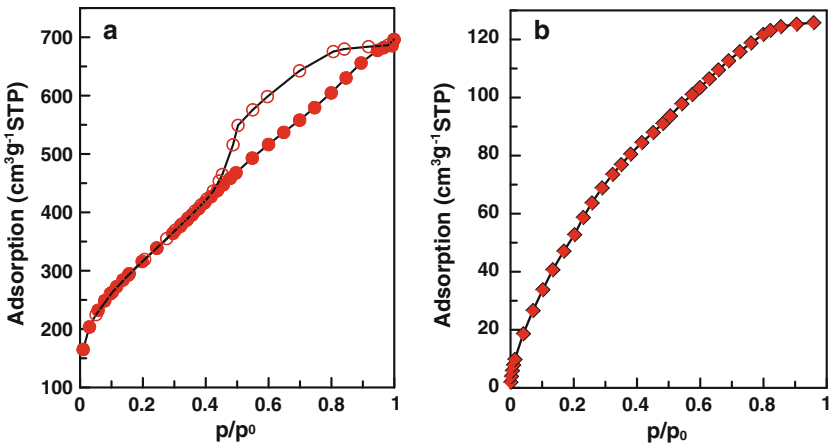

Fig. 1 Nitrogen adsorption (*solid symbols*) and desorption (*open symbols*) isotherms at 77 K (**a**) and *n*-heptane adsorption isotherm at 293 K (**b**) for the silica gel investigated

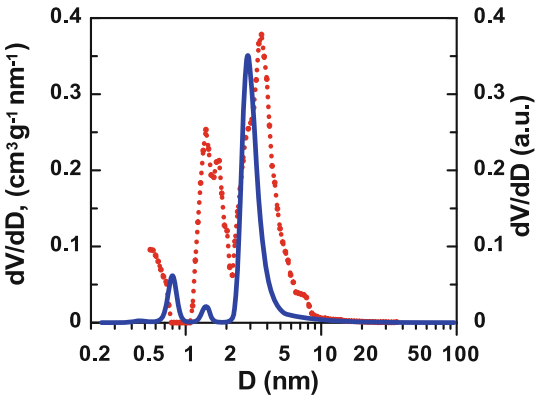

Fig. 2 Pore size distributions derived from low-temperature nitrogen adsorption/desorption data using NLDFT calculations (*dotted line*) and derived from the PALS spectra (*solid line*)

difference between the uptake of *n*-heptane and nitrogen on the investigated silica gel is significant. One can assume that the differences in *n*-heptane and N_2 molecular size and shape, as well as the structure of the adsorbed layer are the main reason for this discrepancy. A steep raise of the N_2 adsorption isotherm at a low relative pressure indicates the presence of micropores, while from *n*-heptane adsorption isotherm one can conclude that this part of the pore system of the investigated silica gel is partially inaccessible for this alkane. Precise knowledge of *n*-heptane adsorption and desorption mechanism may be useful in an appropriate internal pore structure characterization of the investigated silica. Therefore, the PALS which turned out very useful method to investigate the free space evolution during *n*-heptane adsorption and desorption (Zaleski et al. 2012b), was used.

The PSD derived from PALS spectra (Zaleski et al. 2011) measured for the studied samples before *n*-heptane adsorption is also given in Fig. 2. As can be seen PALS and NLDFT methods give similar average pore sizes with a maximum of mesopore diameter near D ~3.5 nm.

The parameters obtained from the analysis of positron annihilation lifetime spectra collected during *n*-heptane adsorption and desorption are presented in Figs. 3, 4, 5, 6. For the studied silica gel—*n*-heptane system the PALS spectra should be divided for five components in order to obtain the acceptable fit in whole range of pressures. Moreover, it is consistent with MELT results obtained for silica gel before *n*-heptane introduction. Two components of a very short lifetime are ascribed to para-positronium (fixed at its known vacuum value 125 ps due to a relatively

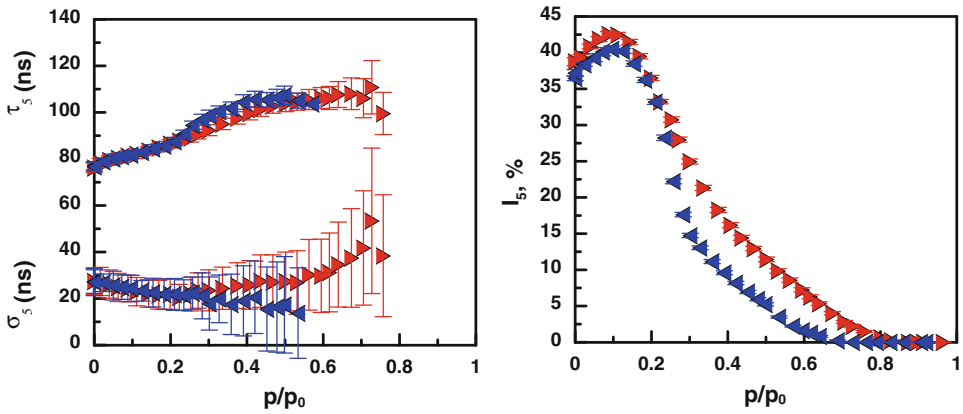

Fig. 3 The lifetime (τ_5), dispersion (σ_5) and intensity (I_5) of the longest-lived component (LLC) as a function of relative *n*-heptane pressure during adsorption (*triangles pointing right*) and desorption (*triangles pointing left*)

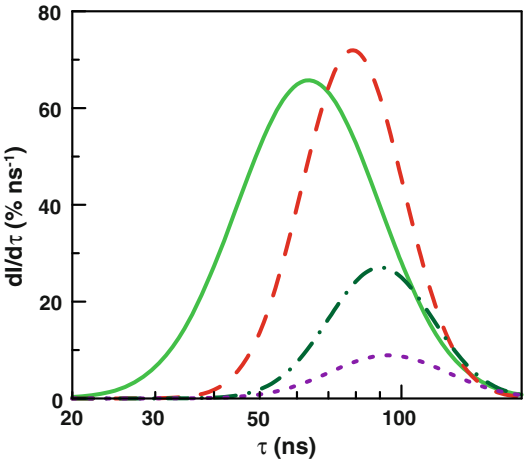

Fig. 4 Change of the distribution intensity in the longest-lived component during *n*-heptane adsorption at $p/p_0 = 0$ (*solid line*), 0.2 (*dashed line*), 0.4 (*dash-dot line*) and 0.6 (*dotted line*)

wide resolution function) and free positron annihilation (changing between about 600 ps for empty pores and 390 ps for pores filled with *n*-heptane). The former one is typically ignored due to great uncertainties and they are therefore ignored in the present discussion. The remaining components are the result of *ortho*-positronium (*o*-Ps) pick-off annihilation and may be ascribed to the groups of pores of various diameters present in the system (Lynn et al. 2003). Their origin is different at various stages of *n*-heptane adsorption or desorption.

Figure 3 shows the lifetime τ_5 and the intensity I_5 of the longest-lived component (LLC) at a various equilibrium pressures of *n*-heptane. The LLC component represents free volume of pores, or, more precisely, the core of pores, when the filling of pores is in progress. At the beginning of the adsorption experiment, i.e. when $p/p_0 = 0$, the component mean lifetime is equal $\tau_5 \approx 76$ ns which corresponds, according to the ETE model (Goworek et al. 1997, Goworek et al. 1998), to $D \approx 4.6$ nm. Lognormal distribution of lifetimes in this component had to be assumed in order to obtain a satisfying fit. Its width estimated as a standard deviation of the distribution is equal $\sigma_5 \approx 27$ ns, what corresponds to the distribution of sizes 2.8–8.4 nm. During adsorption the LLC mean lifetime slightly increases in the whole pressure range, which is accompanied initially by width decrease of the lifetime distribution. The uncertainty of σ_5 becomes quite big at higher pressure, but the standard deviation seems to stabilize. Nevertheless, comparing roughly the constant dispersion σ_5 to the increasing τ_5 we can see that the relative width of lifetime distribution

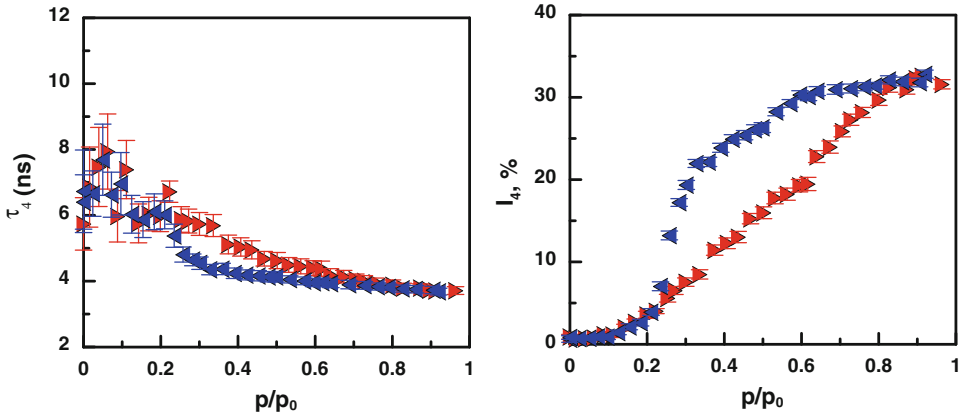

Fig. 5 The lifetime (τ_4) and intensity (I_4) of the medium-lived component (MLC) as a function of relative *n*-heptane pressure during adsorption (*triangles pointing right*) and desorption (*triangles pointing left*)

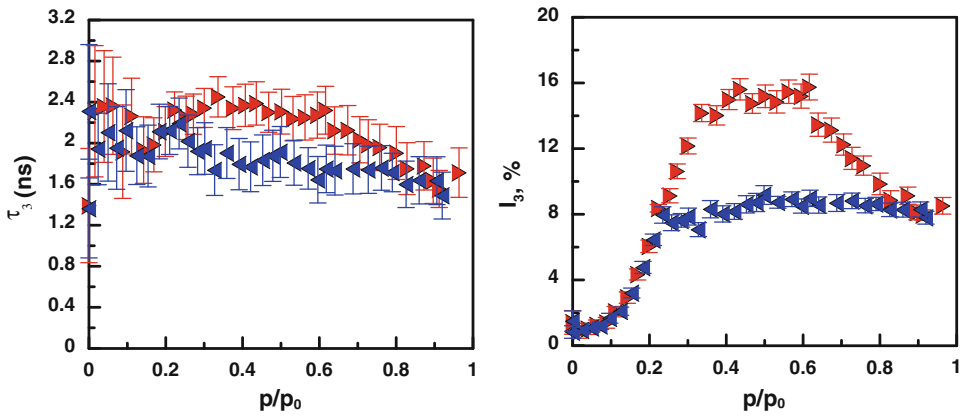

Fig. 6 The SLC lifetime (τ_3) and intensity (I_3) as a function of relative *n*-heptane pressure during adsorption (*triangles pointing right*) and desorption (*triangles pointing left*)

still decreases (Fig. 4). These changes clearly indicate that along with the pressure increase smaller free volumes are filled with *n*-heptane leaving larger ones empty. When the pressure reaches the value $p/p_0 = 0.8$ a low intensity of this component does not allow us to determine mean lifetime and width of lifetime distribution of the LLC with reasonable accuracy. The LLC disappearance is associated with complete filling of all accessible mesopores with *n*-heptane molecules. During desorption a similar but not identical dependence of τ_5 and σ_5 on pressure is observed. Interesting is the fact that at the highest pressure of *n*-heptane both parameters increase along with the decreasing pressure. It reflects the appearance of larger and larger free spaces in *n*-heptane just below the pressure at which emptying of the pores begins. Then, below $p/p_0 = 0.5$ the tendency is the same as during adsorption, but until the pressure reaches $p/p_0 = 0.2$ a hysteresis loop is observed.

In addition the *o*-Ps component intensity changes, which are pronounced in the whole pressure range, provide a valuable information about the mechanism of *n*-heptane adsorption. It is common to assume that this parameter is, as the first approximation, proportional to the relative surface of free volumes constituting porosity of the investigated material. The modifications of pore sizes are highly expected during the adsorption and desorption. At a low pressure LLC intensity increase being attributed to the development of the specific surface inside the pores is observed. It can be assumed that as the pressure increases up to $p/p_0 \approx 10^{-1}$, *n*-heptane molecules are adsorbed onto an accessible surface, first as individual species, and then they form "isle" type structures of various sizes. Therefore, initial development of the surface occurs. When the pressure continues to increase the I_5 intensity (LLC) is decreasing because part of the pores is filled with a liquid due to the capillary condensation. On the basis of the presented pore size distribution (Fig. 2) one can conclude that the pore sizes of this specific silica gel are highly non-uniform. Therefore, it can be expected that during *n*-heptane adsorption fragments of the pore network are filled by n-alkane, while occluded bubbles and empty pore segments are present in the remaining part of the network. Further pressure increase causes collapsing of the bubbles and closing of all free volumes, and as a result the LLC simply disappears, i.e., its intensity becomes negligible. In the pressure range from $p/p_0 = 0.75$ to $p/p_0 = 1$ the LLC intensity is virtually equal zero regardless of the direction of the pressure change. Pressure reduction from $p/p_0 = 0.75$ to $p/p_0 = 0.25$ causes increase of the LLC component intensity. It can be attributed to the successive appearance of free volumes in *n*-heptane filling the silica gel network, according to the interpretation of *o*-Ps intensity mentioned above. It should be emphasized that in this pressure range the hysteresis of the longest-lived *o*-Ps component intensity is evident. In the three-dimensional network of the investigated silica gel pores constrictions and openings can be present. Therefore, in such a network bubble collapse, occurrence or disappearance of empty pore segments are not necessarily reversible. Indeed, the LLC intensity desorption curve goes below the adsorption curve, which proves that lower pressures are required to empty the pores than to fill them. Moreover, it should be noted, that the shape of pressure intensity dependence is similar to the shape of the conventional nitrogen adsorption/desorption isotherm. The difference of the sequence of desorption and adsorption branch of hysteresis in adsorption and PALS experiment is obvious if one takes into account that in the former case the amount of adsorbed nitrogen is measured and in the latter, the free volumes present within the partially filled pores are registered.

Before *n*-heptane loading the medium-lived *o*-Ps component (MLC) probably represents the tail of the pore size distribution corresponding to smaller sizes. It indicates that routinely assumed lognormal distribution of lifetimes in LLC does not perfectly represent the real distribution. However, a very low intensity of this component ($I_4 < 1$ %) shows that the discrepancy is insignificant. Increasing *n*-heptane pressure results in a very distinct, almost linear increase of I_4, which finally reaches the value over 30 % (Fig. 5). Simultaneously, the MLC lifetime heads for $\tau_4 \approx 3.7$ ns, which is characteristic of liquid *n*-heptane at room temperature and under saturation pressure (Zgardzinska and Goworek 2012b). A different behaviour of MLC parameters is observed during desorption, when *n*-heptane removal, indicated by I_4 decrease, starts below $p/p_0 = 0.6$. Then, its decrease at the rate similar to that observed during adsorption is observed. Finally, most of the remaining *n*-heptane, as detected by MLC intensity I_4, is removed in a narrow $p/p_0 = 0.3$–0.2 range. The presence of hysteresis and irreversibility of adsorption in a wide pressure range illustrate continuous condensation and evaporation of the adsorbate. This testifies to the presence in the sample mesopores having different diameters. The shape of the hysteresis loop follows the shape of that recorded in N_2 adsorption experiment. It is worth noting, that the sequence of both branches of hysteresis loop for MLC is the same as in the conventional adsorption experiment.

The shortest-lived component (SLC) represents a group of free volumes of very small sizes (lifetimes τ_3 in the range 1.4–2.5 ns corresponding to 0.36–0.54 nm), which are relatively insensitive to *n*-heptane pressure (Fig. 6). SLC shows a quite similar shape of the hysteresis loop as in the case of MLC, but the sequence of branches representing adsorption and desorption are reversed. During adsorption the I_3 intensity rapidly increases along with the increasing pressure, then becomes stable in the range $p/p_0 = 0.4$–0.6,

and finally decreases along with further pressure increase. When the pressure above the sample decreases the SLC intensity remains stable within the pressure range $p/p_0 = 0.2$–1.0. However, the SLC intensity changes are fully reversible in the range from $p/p_0 = 0.2$ to $p/p_0 = 0$. In the sample without adsorbate at $p/p_0 = 0$ the SLC intensity is still observed ($I_3 \approx 1.4$ %), and can be attributed to the tail of the pore size distribution as in the case of MLC. The hysteresis effect can be explained relatively easily if the observed small free volumes are assigned to the free space between the adsorbed mono- or multilayer and wall of pores. This is confirmed by a rapid increase of I_3 along with the increasing pressure at $p/p_0 < 0.2$ when *n*-heptane layer on the surface of pores is formed. According to this interpretation the intensity decrease of the SLC component may be the result of structural rearrangement of the adsorbate molecules near the interface. This new molecule configuration is sustained during desorption.

The hysteresis observed for SLC pressure dependence demonstrates that the reconstruction of the smallest free spaces is irreversible at decreasing pressure. This is also the result of an unusual type of the porosity in the discussed silica gel, where mesopores of different sizes are "closed" by smaller silica particles of sizes comparable to sizes of small pores between them. The spherical silica particles are the product of SiO_2 nucleation and particle growth in the solution of desired pH. Their sizes are relatively small and of a broad particle size range from 1 to 2 nm (Roberts 2006).

The sizes of the smallest pores determine the evacuation of the adsorbate from pores. Due to small diameters of the external opening of pores, evaporation and desorption take place at a low relative pressure. The specific configuration of silica species in the discussed sample is confirmed by the "triangle" type of the hysteresis in nitrogen adsorption experiment. It is worth noting again that in the adsorption experiment, when the amount of the adsorbate is registered instead of the free volume as in PALS measurement, the sequence of both the adsorption and desorption curve is different than in the case of SLC. Similar effect was observed for LLC component. The present results confirm the differences in the adsorption mechanism in the case of a different type of the pore network. The very narrow openings of pores over larger pores are the main reason that desorption is substantially delayed.

It should be mentioned that for Si-60 which porosity agrees with the type of the pore model: wide openings - narrow pore interior, the hysteresis for all intensity components are close to the result obtained for the isotherm in N_2 adsorption experiment.

The smallest pores represented by the intensity I_3 at $p/p_0 = 0$ due to their extremely low dimensions are inaccessible for adsorbate molecules and remain empty even in the final stage of condensation in the pore interior (Zaleski et al. 2012b). Additionally, small openings cause the formation of plugs or pore blocking at very low pressures and the appearance of the hysteresis loop for $p/p_0 < 0.2$. This effect is not observed in the case of purely mesoporous material with wide openings.

4 Summary

The interpretation of the lifetimes and intensities of the *o*-Ps components derived from PALS spectra can provide a valuable information about the state of the adsorbate phase and the evolution of free volumes at successive stages of pore filling and emptying.

The dependences of *o*-Ps intensities for various groups of pores or free volumes on the pressure exhibit a similar shape of hysteresis as in the conventional adsorption experiment. The long-lived component of *o*-Ps lifetime spectra represent the evolution of free volumes in pore interior. The intensity of the medium-lived component follows satisfactory the amount of *n*-heptane condensed in pores. It reaches the maximum when all pores are completely filled with adsorbate. Some uncertainty is related to the shortest lifetime component. The very short lifetimes represent free volumes of dimension below 1 nm. On the basis of the presented data we suppose that SLC component in PALS experiment represents the free space between the liquid condensate inside pores and silica walls of pores. The rapid change of this component intensity near the saturated pressure may indicate the structural change of the adsorbate film being in contact with the silica surface. This molecular transition is irreversible in a wide pressure range, what results in the appearance of well-defined hysteresis. Part of free volumes represented by SLC should be assigned to the intermolecular voids presented in the silica skeleton. These free volumes are inaccessible of adsorbate molecules. However, their presence is characteristic for amorphous silica materials.

Acknowledgments This work was supported by the Polish Ministry of Science Grant No. NN204 131137. The research was carried out with the equipment purchased thanks to the financial support of the European Regional Development Fund in the framework of the Polish Innovation Economy Operational Program (contract no. POIG.02.01.00-06-024/09 Center of Functional Nanomaterials). We thank Michał Rawski from Center of Functional Nanomaterials for SEM measurements.

References

Brun, M., Lallemand, A., Quinson, J.-F., Eyraud, C.: A new method for the simultaneous determination of the size and shape of pores: the thermoporometry. Thermochim. Acta **21**, 59–88 (1977)

Furtado, F., Galvosas, P., Gonçalves, M., Kopinke, F.-D., Naumov, S., Rodríguez-Reinoso, F., Roland, U., Valiullin, R., Kärger, J.: The evidence of NMR diffusometry on pore space heterogeneity in activated carbon. Micropor. Mesopor. Mater. **141**, 184–191 (2011)

Goworek, J., Stefaniak, W.: Investigation on the porosity of silica gel by thermal desorption of liquids. Mater. Chem. Phys. **82**, 244–248 (1992)

Goworek, J., Stefaniak, W.: Investigation of heavy-ion-produced pore defects in organic foil by thermal desorption of liquids. Colloids Surf. **82**, 71–75 (1994)

Goworek, J., Zaleski, R., Buda, W., Kierys, A.: Free volumes evolution during desorption of *n*-heptane from silica with regular pore geometry. Positron annihilation study. Appl. Surf. Sci. **256**, 5316–5322 (2010)

Goworek, T., Ciesielski, K., Jasińska, B., Wawryszczuk, J.: Positronium in large voids. Silicagel. Chem. Phys. Lett. **272**, 91–95 (1997)

Goworek, T., Ciesielski, K., Jasińska, B., Wawryszczuk, J.: Positronium states in the pores of silica gel. Chem. Phys. **230**, 305–315 (1998)

Halasz, I., Kierys, A., Goworek, J., Liu, H., Patterson, R.E.: 29Si NMR and Raman glimpses into the molecular structures of acid and base set silica gels obtained from TEOS and Na-silicate. J. Phys. Chem. C **115**, 24788–24799 (2011)

He, C., Oka, T., Kobayashi, Y., Oshima, N., Ohdaira, T., Kinomura, A., Suzuki, R.: Positronium annihilation and pore surface chemistry in mesoporous silica films. Appl. Phys. Lett. **91**, 024102 (2007)

Kansy, J.: Microcomputer program for analysis of positron annihilation lifetime spectra. Nucl. Instrum. Methods Phys. Res. Sect. A **374**, 235–244 (1996)

Koshimizu, M., Shimokita, K., Zhou, H.S., Honma, I., Asai, K.: Positron annihilation lifetime in ordered porous silica SBA-3. J. Phys. Chem. C **112**, 8779–8783 (2008)

Krause, J., Schrage, Ch., Schuy, A., Woike, Th, Kockrick, E., Kaskel, S., Schaniel, D.: Effect of synthesis conditions on porous structure, luminescence and absorption properties of dye-loaded silica xerogels. Micropor. Mesopor. Mater. **142**, 245–250 (2011)

Kullmann, J., Enke, D., Thraenert, S., Krause-Rehberg, R., Inayat, A.: Characterization of nanoporous monoliths using nitrogen adsorption and positronium annihilation lifetime spectroscopy. Colloids Surf. A **357**, 17–20 (2010)

Lynn, K.G., Weber, M.H.: Positron porosimetry. In: Jean, Y.C., Mallon, P.E., Schrader, D.M. (eds.) Principles and Applications of Positron and Positronium Chemistry, p. 167. World Scientific, Singapore (2003)

Pikus, S., Celer, E.B., Jaroniec, M., Solovyov, L.A., Kozak, M.: Studies of intrawall porosity in the hexagonally ordered mesostructures of SBA-15 by small angle X-ray scattering and nitrogen adsorption. Appl. Surf. Sci. **256**, 5311–5315 (2010)

Roberts, W.O.: Manufacturing and applications of water-borne colloidal silica. In: Bergna, H.E., Roberts, W.O. (eds.) Colloidal Silica Fundamentals and Applications, vol. 131, pp. 131–175. CRC Press, Taylor & Francis, Boca Raton (2006)

Schüth, F., Sing, K.S.W., Weitkamp, J. (eds.): Handbook of Porous Solids, vol. 1. Wiley-VCH, Weinheim (2002)

Shukla, A., Peter, M., Hoffmann, L.: Analysis of positron lifetime spectra using quantified maximum entropy and a general linear filter. Nucl. Instrum. Methods Phys. Res. Sect. A **335**, 310–317 (1993)

Smarsly, B., Göltner, Ch., Antonietti, M., Ruland, W., Hoinkis, E.: SANS investigation of nitrogen sorption in porous silica. J. Phys. Chem. B. **105**, 831–884 (2001)

Thraenert, S., Hassan, E.M., Enke, D., Fuerst, D., Krause-Rehberg, R.: Verifying the RTE model: *ortho*-positronium lifetime measurement on controlled pore glasses. Phys. Status Solidi C **4**(10), 3819–3822 (2007)

Zaleski, R., Borówka, A., Wawryszczuk, J., Goworek, J., Goworek, T.: Positron probing of the micellar template interior in MCM-41. Chem. Phys. Lett. **372**, 794–799 (2003)

Zaleski, R.: Measurement and analysis of the positron annihilation lifetime spectra for mesoporous silica. Acta Phys. Polon. A **110**, 729–738 (2006)

Zaleski, R., Kierys, A., Grochowicz, M., Dziadosz, M., Goworek, J.: Synthesis and characterization of nanostructural polymer–silica composite: positron annihilation lifetime spectroscopy study. J. Colloids Interf. Sci. **358**, 268–276 (2011)

Zaleski, R., Kierys, A., Dziadosz, M., Goworek, J., Halasz, I.: Positron annihilation and N2 adsorption for nanopore determination in silicapolymer composites. RSC Adv. **2**, 3729–3734 (2012a)

Zaleski, R., Dolecki, W., Kierys, A., Goworek, J.: n-heptane adsorption and desorption on porous silica observed by positron annihilation lifetime spectroscopy. Micropor. Mesopor. Mater. **154**, 142–147 (2012b)

Zgardzińska, B., Goworek, T.: Positronium in solid phases of methanol. Chem. Phys. Lett. **501**, 44–46 (2010)

Zgardzińska, B., Goworek, T.: Positronium in alkanes. From neat nonadecane to wax. Chem. Phys. Lett. **547**, 35–37 (2012a)

Zgardzińska, B., Goworek, T.: Positronium bubble in liquid alkanes and alcohols. Chem. Phys. **405**, 32–39 (2012b)